Voltage-Controlled Skyrmion Memristor for Energy-Efficient Synapse Applications

Shijiang Luo, Nuo Xu, *Member, IEEE*, Zhe Guo, Yue Zhang, Jeongmin Hong, and Long You, *Member, IEEE*

***Abstract*— A novel voltage-controlled skyrmion memristor (VCSK-Memristor) based on a multiferroic heterostructure is proposed and studied. Under electric-field-modulated magnetic anisotropy via remnant strain, continuously tunable resistance is obtained in a VCSK-Memristor due to the skyrmion size modulation in the ferromagnetic layer. Geometrical scaling studies on VCSK-Memristor are performed to provide the guidelines for the design and optimization of this newly proposed spintronic device. The results indicate that the VCSK-Memristor is advantageous for fabricating energy-efficient synapse arrays for hardware neural-network applications.**

***Index Terms*— Skyrmion, spintronics, memristor, synapse, multiferroic heterostructure, magnetic tunnel junction.**

I. Introduction

DYNAMIC energy is considered as one of the most critical challenges for the continuing miniaturization of spintronic devices. One promising solution is to manipulate the magnetization in ferromagnetic (FM) materials using electric fields/voltages instead of magnetic fields or spin-torques produced by power-dissipating currents [1]. Electric field-modulated magnetization via remnant strain has been demonstrated in FM/ferroelectric (FE) multiferroic heterostructures [2]. The strain and the magnetization change are retained after removing the electric field and reversible under non-180° FE polarization switching [2]. Furthermore, continuously tunable remnant strain values in FE layer can be achieved by properly applying electric field from the polarized state [3]. Therefore, it is expected to continuously tune the magnetization via "non-volatile" remnant strain.

Magnetic skyrmions are topological spin textures with non-linear configuration in FM films [4], [5]. Current-driven skyrmion motion with assistance of electric fields has been studied [6], [7], where electric fields are used to control whether the skyrmion passes the control region or not but have little direct effect on the skyrmion itself, and the skyrmion is considered as a rigid quasi-particle, having an achiral magnetization vector field. Although the small footprint and topological stability features of skyrmions are very much valued for bi-stable non-volatile memory (NVM) applications (*e.g.* skyrmion racetrack memory [8]), an unexplored topic in this field is to re-investigate the skyrmion's feature for memristive devices, which takes advantages of skyrmion's size modulation resulted continuous resistance change.

In this work, a novel multiferroic heterostructure is proposed with skyrmions induced in the FM layer, whose size is simply modulated by electric field control of magnetic anisotropy via remnant strain. The continuous change of magnetization is later read out through tunneling magneto-resistance (TMR). Therefore, a new class of spintronic devices is proposed as the voltage-controlled skyrmion memristor (VCSK-Memristor).

Manuscript received January 26, 2019; accepted February 4, 2019. Date of publication February 11, 2019; date of current version April 2, 2019. This work was supported by the National Natural Science Foundation of China under Grant 61674062 and Grant 61821003. The review of this letter was arranged by Editor E. A. Gutiérrez-D. *(Corresponding author: Long You.)*

S. Luo, Z. Guo, Y. Zhang, J. Hong, and L. You are with the School of Optical and Electronic Information, Huazhong University of Science and Technology, Wuhan 430074, China (e-mail: lyou@hust.edu.cn).

N. Xu is with the Department of Electrical Engineering and Computer Sciences, University of California at Berkeley, Berkeley, CA 94720 USA.

Color versions of one or more of the figures in this letter are available online at http://ieeexplore.ieee.org.

Digital Object Identifier 10.1109/LED.2019.2898275

II. Device Structure and Simulation Methods

The basic concept of the VCSK-Memristor based on a multiferroic heterostructure consisting of FE/heavy metal (HM)/FM layers is depicted in Fig. 1a. A skyrmion can be initiated and stabilized at the center of the FM layer by injection of spin polarized current through a magnetic tunnel junction (MTJ) structure [9], [10]. Such MTJ devices with FE substrate have been investigated for strain-assisted magnetization switching for memory application [11], [12]. In our case, once a voltage is applied to the FE layer, a strain is generated and further transferred to the coupled FM layer, causing skyrmion size modulated. After applied voltage is removed, remnant strain is retained due to the preservation of non-180° FE polarization switching [2], [3] so as for the magnetization change of the FM layer. When using MTJ to read out the TMR, depending on the fraction of the reversed domain (*i.e.* skyrmion region), a continuous range of resistance values can be sensed.

A heterostructure with (011) PMN-PT/$[Co/Pt]_n$ layers are simulated herein. $[Co/Pt]_n$ multilayer with perpendicular magnetic anisotropy (PMA) and *Dzyaloshinskii–Moriya* interaction (DMI) is used as the medium for inducing skyrmions [13], while electric filed control of magnetization in (011) PMN-PT/$[Co/Pt]_n$ has also been demonstrated [14], [15]. Magnetic [9] and elastic [16], [17] parameters of $[Co/Pt]_n$ used in simulation are listed in Table I. In addition, lead-free materials may also be exploited to equally work as the FE layer, *e.g.* $BaTiO_3$ [18].

Magnetization dynamics in the FM layer are simulated by solving the *Landau-Lifshitz-Gilbert* (LLG) equation under micro-magnetics scheme [19], in which the energy density

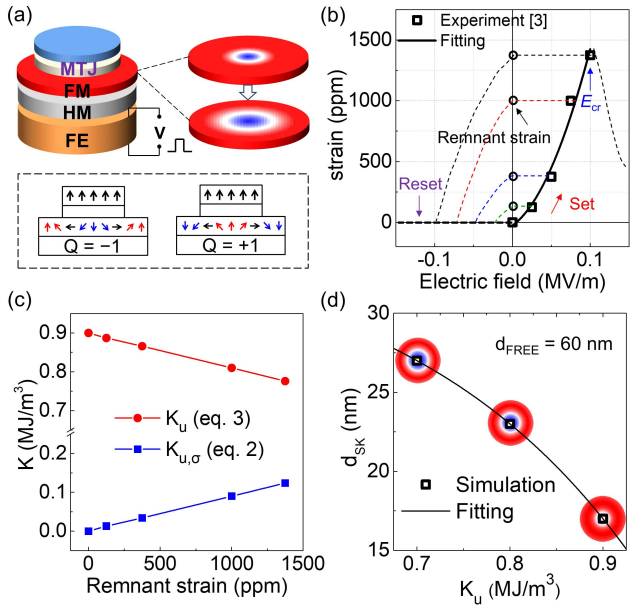

Fig. 1. (a) Schematics of a voltage-controlled skyrmion memristor. A skyrmion can exist in two states with a skyrmion number $Q = -1$ or $+1$. (b) Strain response of (011) PMN-PT under electric field. (c) Perpendicular magnetic anisotropy constant (K_u) and stress-induced anisotropy constant ($K_{u,\sigma}$) under different remnant strain. (d) Skyrmion diameter (d_{SK}) and snapshots of FM layer under different K_u.

TABLE I
SIMULATION PARAMETERS OF $[Co/Pt]_N$

Parameters		Values
Magnetic [9]	Saturation magnetization, M_S	580 kA/m
	Initial PMA constant, K_{u0}	0.9 MJ/m^3
	DMI constant, D	3.0 mJ/m^2
	Exchange constant, A_{ex}	10 pJ/m
	Gilbert damping constant, α	0.3
Elastic [16], [17]	Magnetostriction constant, λ	290 ppm
	Young's Modulus, Y	180 GPa
	Poisson's ratio, ν	0.31
Geometric [9]	Simulation mesh size (one site in thickness direction)	$1 \times 1 \times 1$ nm^3

consists of PMA (E_k), exchange, DMI, and demagnetization effects. The relationship between the strain (ε) in FE layer and applied electric field (E) is extracted from experiment results of (011) PMN-PT [3], as shown in Fig. 1b. From a polarized state (referring to zero strain), E below the critical value (E_{cr}, ~0.1 MV/m, where a strain jump peak occurs) can cause the non-180° FE polarization switching and set a remnant strain value (ε_r). Different ε_r depends on the proportion of the switched non-180° FE polarization controlled by amplitude of E, and quasi-continuous ε_r (from 0 to ~1375 ppm) is expected. A reversed electric field can switch FE layer to the initial polarized state, denoted as the Reset operation.

The associated stress (σ) produced by the remnant strain that acts on FM layer is described by *Hooke*'s Law [20]

$$\sigma = \frac{Y}{1-\nu^2}\varepsilon_r, \tag{1}$$

with stress-induced anisotropy $K_{u,\sigma}$ evaluated by [16]

$$K_{u,\sigma} = -\frac{3}{2}\lambda\sigma. \tag{2}$$

The overall PMA constant K_u, which relates to E_k in micromagnetic simulations, is expressed as

$$K_u = K_{u0} + K_{u,\sigma}. \tag{3}$$

Figure 1c shows resulted K_u variation under different ε_r according to eqs. (1)–(3), to justify that the strain induced PMA tuning is achievable in this multiferroic heterostructure. A larger K_u would shrink the size of a skyrmion, since it favors a stronger PMA to dominate the total energy terms, which is reflected on the skyrmion diameter (d_{SK}, defined as the spacing of intercepts of $m_z = 0$) *vs.* K_u curves as shown in Fig. 1d. Thus, when E varies from 0 to 0.1 MV/m (accordingly, K_u changes from 0.9 to 0.78 MJ/m^3), the resulted d_{SK} has a range from 17 to 24 nm in an FM layer with diameter (d_{FREE}) of 60 nm. Therefore, it is proved that d_{SK} can be modulated by the applied voltage in the FE layer.

As a proof-of-concept, the strain-mediated effect model has been used for capturing the electric field modulation of magnetization. In practical applications, with various effects involved, such as interface [14] and charge effects [21], a same E value to induce a lager variation on K_u is expected. On the other hand, the strain may also change other magnetic properties such as DMI constant (D), saturation magnetization (M_S). However, previous studies show that, in Co/Pt-based material systems, D variation is just 0.2% by up to 0.1% strain [22], and M_S is almost unchanged under strain [15]; whereas magnetic anisotropy could change significantly, even for a large rotation between out-of-plane and in-plane directions [14]. Thus, the strain-induced variation of D and M_S is neglected in this work.

III. VCSK MEMRISTOR OPERATIONS AND PERFORMANCE

The tunneling resistance (R) of an MTJ can be expressed as

$$R = R_P + \frac{1}{2}(R_{AP} - R_P)(1 - \cos\theta) \tag{4}$$

where P and AP refer to parallel (P) and antiparallel (AP) states, respectively, and θ is the magnetization angle between fixed and free layers [23]. In this work, a skyrmion can exist in the free layer in two states with a skyrmion number [24], [25] $Q = -1$ and $+1$ to identify the core of skyrmion pointing downward and upward, respectively (Fig. 1a). The normalized perpendicular component of magnetization (m_z) in the free layer beneath the fixed layer is calculated from simulation data as $\cos\theta$ when magnetization in the fixed layer lies upward. The diameter (d_{FIX}) of fixed layer can be varied to obtain different m_z and therefore different ranges for resistance tuning.

The normalized resistance R/R_P versus d_{SK} is then calculated and shown in Fig. 2a, where a TMR ($= (R_{AP} - R_P)/R_P$) of 200% [26] is assumed. The electric field induced resistance modulation (ΔR) is shown in Fig. 2b. Clearly, the resistance can be effectively controlled by the applied voltage in a large range, enabling this device to be functioned as a memristor [27]. To well sense the continuous change of the skyrmion size and the dynamic resistance range, an MTJ with higher TMR is preferred, along with stronger electric field controlled-magnetization effect to induce larger skyrmion size variation. On the other hand, two skyrmion states are

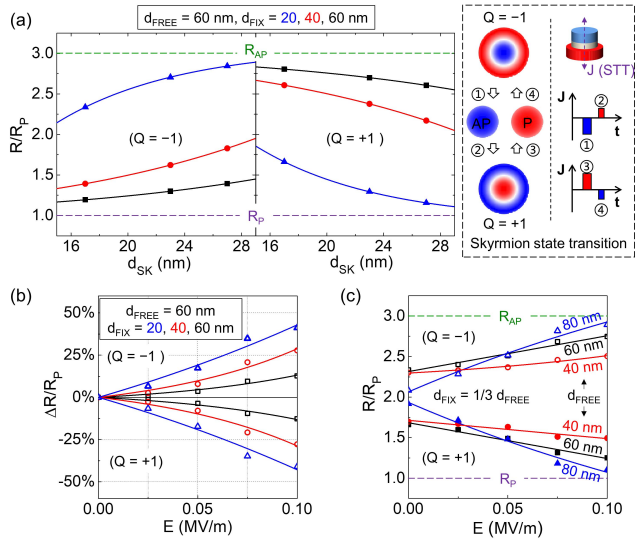

Fig. 2. (a) Normalized resistance R/R_P as a function of d_{SK} under different d_{FIX} at d_{FREE} = 60 nm and illustration of the transition of two skyrmion states via STT. (b) Electric field (E) induced resistance modulation (ΔR). (c) R/R_P as a function of E in VCSK-Memristor with different d_{FREE}. TMR = 200% is assumed during the calculation.

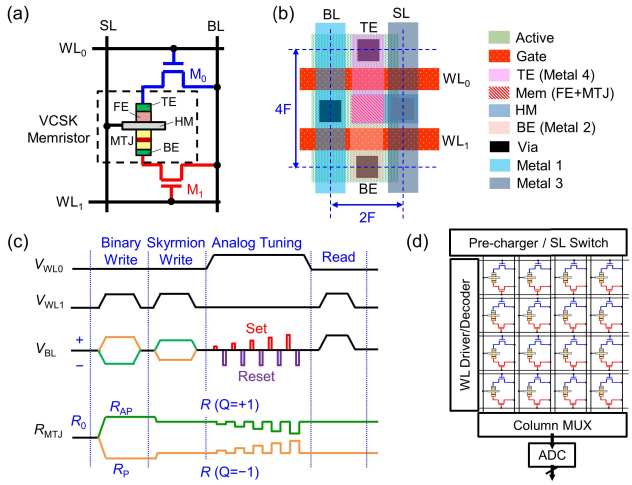

Fig. 3. (a) Illustration of a 2T1M VCSK-based synapse cell. (b) Layout design with a cell size of $8F^2$. (c) Schematic of operations and sequence diagram. (d) Synaptic core array and periphery circuit designs.

transferrable to each other by applying programming current pulses through the MTJ via spin transfer torque (STT) [10] (Fig. 2a). Hence, two separate levels of resistance values (*i.e.* both the cases of $Q = -1$ and $+1$) can be implemented within one device. Note that the application of current-induced STT would produce transient *Joule* heating, while an experiment study demonstrated that skyrmion state is preferred and stable under thermal activation in skyrmion-based material system [28].

VCSK-Memristor is a nano-pillar structure with its planar area equal to the FM free layer. The devices with different sizes from 80 to 40 nm are investigated to evaluate their scaling potentials for high-density array applications. Comparable resistance tuning capabilities are found as shown in Fig. 2c, which ensures the scalability of the proposed device. However, there exists a design trade-off between the device's size and dynamic resistance range, which is due to the enhanced boundary repulsion effect on skyrmion expansion (i.e. reduced tunability of skyrmion size) at reduced size.

The non-volatility (*i.e.* retention) is determined by the remnant strain, which as shown in [3], can be stable up to days and has no significant degradation under enduring voltage cycles. However, the application of periodic strain cycling may generate the pinholes resulting in the degradation of TMR, to avoid which, future applications need to determine the optimal range of strain induced. The program (write) speed of VCSK-memristor is determined by FE polarization switching in FE layer (for fast switching, can be <10 ns [29]), while the read time is similar to existing MRAMs (<20 ns [30]). Due to the non-volatile property, the power consumption is dominated by dynamic voltage-induced FE polarization switching process. For a full-swing switching, the power can be estimated as $P_rSV/2$ [29], where P_r (30 μC/cm^2 [3]) is the remnant polarization, S the area, and V the voltage amplitude. Providing our device with 60 nm diameter and 100 nm FE thickness, a voltage of $V = 0.1\text{MV/m} \times 100\text{nm} = 10$ mV corresponds to an ultra-low energy consumption of ~5 aJ per operation. This energy consumption is drastically lower compared with that of ReRAM (~0.1 pJ) and PCM (~10 pJ) based memristors [31].

IV. VCSK-Based Synapse Design

Memristor technologies have been exploited as synapse-like functions for self-adaptive networks [32]. The 3-terminal VCSK-Memristor can be used for synapse applications with its read-out resistance as the synapse weight. Figure 3a and b show the VCSK-based synapse cell and layout design with the size of $8F^2$ (F: feature size). A standard synapse cell consists of two transistors (M_0, M_1) and a VCSK-Memristor, connected by Word lines (WL_0, WL_1), Bit line (BL), and Source line (SL) in back-end-of-line (BEOL) layers. During each programing cycle, M_0 is turned on to apply the voltage pulse on the FE layer, while M_1 is selected during each read cycle. The overall operations are summarized in Fig. 3c. With WL_1 voltage (V_{WL1}) on and WL_0 voltage (V_{WL0}) off, two skyrmion states could be selected by programing the BL voltage (V_{BL}). With V_{WL0} on and V_{WL1} off, the desired MTJ resistance can be set by applying V_{BL} with different amplitude after Reset operation. A small V_{BL} is used to perform the Read operation. Compared with existing proposals of skyrmion-based synapses [33], [34], which use current-induced spin orbit torque (SOT) to drive skyrmion motion and require a large footprint and power consumption (due to self-heating effect), VCSK-based synapse cell is advantageous for fabricating high-density and energy-efficient array, as illustrated in Fig. 3d.

V. Conclusion

A VCSK-Memristor of FE/HM/MTJ structure is proposed. Physics-based simulations suggest that the readout resistance values can be efficiently modulated by applying voltage as well as the assistance of STT. Geometry scaling studies further reveal that the memristive behavior is available for this new device with different size, guaranteeing its robustness under process variability. The VCSK-Memristor cells have a promising potential to fabricate energy-efficient synapse arrays for constructing hardware neuromorphic networks.

REFERENCES

[1] F. Matsukura, Y. Tokura, and H. Ohno, "Control of magnetism by electric fields," *Nature Nanotechnol.*, vol. 10, no. 3, pp. 209–220, Mar. 2015. doi: 10.1038/nnano.2015.22.

[2] T. Wu, A. Bur, P. Zhao, K. P. Mohanchandra, K. Wong, K. L. Wang, C. S. Lynch, and G. P. Carman, "Giant electric-field-induced reversible and permanent magnetization reorientation on magnetoelectric Ni/(011) $[Pb(Mg_{1/3}Nb_{2/3})O3]_{(1-x)}$-$[PbTiO_3]_x$ heterostructure," *Appl. Phys. Lett.*, vol. 98, no. 1, 2011, Art. no. 012504. doi: 10.1063/1.3534788.

[3] T. Wu, P. Zhao, M. Bao, A. Bur, J. L. Hockel, K. Wong, K. P. Mohanchandra, C. S. Lynch, and G. P. Carman, "Domain engineered switchable strain states in ferroelectric (011) $[Pb(Mg_{1/3}Nb_{2/3})O_3]_{(1-x)}$-$[PbTiO_3]_x$ (PMN-PT, x≈0.32) single crystals," *J. Appl. Phys.*, vol. 109, no. 12, 2011, Art. no. 124101. doi: 10.1063/1.3595670.

[4] W. Kang, Y. Huang, X. Zhang, Y. Zhou, and W. Zhao, "Skyrmion-electronics: An overview and outlook," *Proc. IEEE.*, vol. 104, no. 10, pp. 2040–2061, Oct. 2016. doi: 10.1109/JPROC.2016.2591578.

[5] W. Jiang, G. Chen, K. Liu, J. Zang, S. G. E. T. Velthuis, and A. Hoffmann, "Skyrmions in magnetic multilayers," *Phys. Rep.*, vol. 704, pp. 1–49, Aug. 2017. doi: 10.1016/j.physrep.2017.08.001.

[6] P. Upadhyaya, G. Yu, P. K. Amiri, and K. L. Wang, "Electric-field guiding of magnetic skyrmions," *Phys. Rev. B, Condens. Matter*, vol. 92, no. 13, 2015, Art. no. 134411. doi: 10.1103/PhysRevB.92.134411.

[7] S. Luo, M. Song, X. Li, Y. Zhang, J. Hong, X. Yang, X. Zou, N. Xu, and L. You, "Reconfigurable skyrmion logic gates," *Nano Lett.*, vol. 18, no. 2, pp. 1180–1184, Feb. 2018. doi: 10.1021/acs.nanolett.7b04722.

[8] D. Zhu, W. Kang, S. Li, Y. Huang, X. Zhang, Y. Zhou, and W. Zhao, "Skyrmion racetrack memory with random information update/deletion/insertion," *IEEE Trans. Electron Devices*, vol. 65, no. 1, pp. 87–95, Jan. 2018. doi: 10.1109/TED.2017.2769672.

[9] J. Sampaio, V. Cros, S. Rohart, A. Thiaville, and A. Fert, "Nucleation, stability and current-induced motion of isolated magnetic skyrmions in nanostructures," *Nature Nanotechnol.*, vol. 8, no. 11, pp. 839–844, Nov. 2013. doi: 10.1038/nnano.2013.210.

[10] X. Zhang, W. Cai, X. Zhang, Z. Wang, Z. Li, Y. Zhang, K. Cao, N. Lei, W. Kang, Y. Zhang, H. Yu, Y. Zhou, and W. Zhao, "Skyrmions in magnetic tunnel junctions," *ACS Appl. Mater. Interfaces*, vol. 10, no. 19, pp. 16887–16892, May 2018. doi: 10.1021/acsami.8b03812.

[11] A. Khan, D. E. Nikonov, S. Manipatruni, T. Ghani, and I. A. Young, "Voltage induced magnetostrictive switching of nanomagnets: Strain assisted strain transfer torque random access memory," *Appl. Phys. Lett.*, vol. 104, no. 26, Jul. 2014, Art. no. 262407. doi: 10.1063/1.4884419.

[12] Z. Zhao, M. Jamali, N. D'Souza, D. Zhang, S. Bandyopadhyay, J. Atulasimha, and J.-P. Wang, "Giant voltage manipulation of MgO-based magnetic tunnel junctions via localized anisotropic strain: A potential pathway to ultra-energy-efficient memory technology," *Appl. Phys. Lett.*, vol. 109, no. 9, Aug. 2016, Art. no. 092403. doi: 10.1063/1.4961670.

[13] S. Woo, K. Litzius, B. Krüger, M.-Y. Im, L. Caretta, K. Richter, M. Mann, A. Krone, R. M. Reeve, M. Weigand, P. Agrawal, I. Lemesh, M.-A. Mawass, P. Fischer, M. Kläui, and G. S. D. Beach, "Observation of room-temperature magnetic skyrmions and their current-driven dynamics in ultrathin metallic ferromagnets," *Nature Mater.*, vol. 15, no. 5, pp. 501–506, May 2016. doi: 10.1038/nmat4593.

[14] B. Peng, Z. Zhou, T. Nan, G. Dong, M. Feng, Q. Yang, X. Wang, S. Zhao, D. Xian, Z. D. Jiang, W. Ren, Z. G. Ye, N. X. Sun, and M. Liu, "Deterministic switching of perpendicular magnetic anisotropy by voltage control of spin reorientation transition in $(Co/Pt)_3/Pb(Mg_{1/3}Nb_{2/3})O_3$-$PbTiO_3$ multiferroic heterostructures," *ACS Nano*, vol. 11, no. 4, pp. 4337–4345, Apr. 2017. doi: 10.1021/acsnano.7b01547.

[15] Y. Sun, Y. Ba, A. Chen, W. He, W. Wang, X. Zheng, L. Zou, Y. Zhang, Q. Yang, L. Yan, C. Feng, Q. Zhang, J. Cai, W. Wu, M. Liu, L. Gu, Z. Cheng, C.-W. Nan, Z. Qiu, Y. Wu, J. Li, and Y. Zhao, "electric-field modulation of interface magnetic anisotropy and spin reorientation transition in $(Co/Pt)_3$/PMN–PT heterostructure," *ACS Appl. Mater. Interfaces*, vol. 9, no. 12, pp. 10855–10864, Mar. 2017. doi: 10.1021/acsami.7b00284.

[16] K. Kyuno, J.-G. Ha, R. Yamamoto, and S. Asano, "Theoretical study on the strain dependence of the magnetic anisotropy of X/Co(X=Pt, Cu, Ag, and Au) metallic multilayers," *J. Appl. Phys.*, vol. 79, no. 9, pp. 7084–7089, 1996. doi: 10.1063/1.361476.

[17] E. A. M. van Alphen, S. G. E. te Velthuis, H. A. M. de Gronckel, K. Kopinga, and W. J. M. de Jonge, "NMR study of the strain in Co-based multilayers," *Phys. Rev. B, Condens. Matter*, vol. 49, no. 24, pp. 17336–17341, Jun. 1994. doi: 10.1103/PhysRevB.49.17336.

[18] S. Geprägs, A. Brandlmaier, M. Opel, R. Gross, and S. T. B. Goennenwein, "Electric field controlled manipulation of the magnetization in Ni/$BaTiO_3$ hybrid structures," *Appl. Phys. Lett.*, vol. 96, no. 14, Apr. 2010, Art. no. 142509. doi: 10.1063/1.3377923.

[19] M. J. Donahue and D. G. Porter, "OOMMF: Object oriented micromagnetic framework," Nat. Inst. Standards Technol., Gaithersburg, MD, USA, Tech. Rep. NISTIR 6376, Jan. 1999. [Online]. Available: http://math.nist.gov/oommf

[20] D. Wang, C. Nordman, Z. Qian, J. M. Daughton, and J. Myers, "Magnetostriction effect of amorphous CoFeB thin films and application in spin-dependent tunnel junctions," *J. Appl. Phys.*, vol. 97, no. 10, May 2005, Art. no. 10C906. doi: 10.1063/1.1848355.

[21] T. Nan, Z. Zhou, M. Liu, X. Yang, Y. Gao, B. A. Assaf, H. Lin, S. Velu, X. Wang, H. Luo, J. Chen, S. Akhtar, E. Hu, R. Rajiv, K. Krishnan, S. Sreedhar, D. Heiman, B. M. Howe, G. J. Brown, and N. X. Sun, "Quantification of strain and charge co-mediated magneto-electric coupling on ultra-thin Permalloy/PMN-PT interface," *Sci. Rep.*, vol. 4, Jan. 2014, Art. no. 3688. doi: 10.1038/srep03688.

[22] P. M. Shepley, G. Burnell, and T. A. Moore, "Domain wall energy and strain in Pt/Co/Ir thin films on piezoelectric transducers," *J. Phys., Condens. Matter*, vol. 30, no. 34, Jul. 2018, Art. no. 344002. doi: 10.1088/1361-648X/aad3a2.

[23] Y. Zhang, B. Yan, J. Ou-Yang, X. Wang, B. Zhu, S. Chen, and X. Yang, "Significant manipulation of output performance of a bridge-structured spin valve magnetoresistance sensor via an electric field," *J. Appl. Phys.*, vol. 119, no. 4, Jan. 2016, Art. no. 044101. doi: 10.1063/1.4940360.

[24] N. Nagaosa and Y. Tokura, "Topological properties and dynamics of magnetic skyrmions," *Nature Nanotechnol.*, vol. 8, no. 12, pp. 899–911, Dec. 2013. doi: 10.1038/nnano.2013.243.

[25] Y. Zhang, S. Luo, B. Yan, J. Ou-Yang, X. Yang, S. Chen, B. Zhu, and L. You, "Magnetic skyrmions without the skyrmion Hall effect in a magnetic nanotrack with perpendicular anisotropy," *Nanoscale*, vol. 9, no. 29, pp. 10212–10218, Jul. 2017. doi: 10.1039/c7nr01980g.

[26] Y. J. Song, J. H. Lee, H. C. Shin, K. H. Lee, K. Suh, J. R. Kang, S. S. Pyo, H. T. Jung, S. H. Hwang, G. H. Koh, S. C. Oh, S. O. Park, J. K. Kim, J. C. Park, J. Kim, K. H. Hwang, G. T. Jeong, K. P. Lee, and E. S. Jung, "Highly functional and reliable 8 Mb STT-MRAM embedded in 28 nm logic," in *IEDM Tech. Dig.*, Dec. 2016, pp. 27.2.1–27.2.4. doi: 10.1109/IEDM.2016.7838491.

[27] L. O. Chua, "Memristor-the missing circuit element," *IEEE Trans. Circuit Theory*, vol. CT-18, no. 5, pp. 507–519, Sep. 1971. doi: 10.1109/TCT.1971.1083337.

[28] I. Lemesh, K. Litzius, M. Böttcher, P. Bassirian, N. Kerber, D. Heinze, J. Zázvorka, F. Büttner, L. Caretta, M. Mann, M. Weigand, S. Finizio, J. Raabe, M.-Y. Im, H. Stoll, G. Schütz, B. Dupé, M. Kläui, and G. S. D. Beach, "Current-induced skyrmion generation through morphological thermal transitions in chiral ferromagnetic heterostructures," *Adv. Mater.*, vol. 30, no. 49, Oct. 2018, Art. no. 1805461. doi: 10.1002/adma.201805461.

[29] J.-M. Hu, Z. Li, L.-Q. Chen, and C.-W. Nan, "High-density magnetoresistive random access memory operating at ultralow voltage at room temperature," *Nature Commun.*, vol. 2, Nov. 2011, Art. no. 553. doi: 10.1038/ncomms1564.

[30] N. Xu, Y. Lu, W. Qi, Z. Jiang, X. Peng, F. Chen, J. Wang, W. Choi, S. Yu, and D. S. Kim, "STT-MRAM design technology co-optimization for hardware neural networks," in *IEDM Tech. Dig.*, Dec. 2018, pp. 15.3.1–15.3.4.

[31] S. Yu and P.-Y. Chen, "Emerging memory technologies: Recent trends and prospects," *IEEE Solid-State Circuits Mag.*, vol. 8, no. 2, pp. 43–56, Mar. 2016. doi: 10.1109/mssc.2016.2546199.

[32] S. H. Jo, T. Chang, I. Ebong, B. B. Bhadviya, P. Mazumder, and W. Lu, "Nanoscale memristor device as synapse in neuromorphic systems," *Nano Lett.*, vol. 10, no. 4, pp. 1297–1301, Apr. 2010. doi: 10.1021/nl904092h.

[33] M.-C. Chen, A. Sengupta, and K. Roy, "Magnetic skyrmion as a spintronic deep learning spiking neuron processor," *IEEE Trans. Magn.*, vol. 54, no. 8, Aug. 2018, Art. no. 1500207. doi: 10.1109/TMAG.2018.2845890.

[34] Y. Huang, W. Kang, X. Zhang, Y. Zhou, and W. Zhao, "Magnetic skyrmion-based synaptic devices," *Nanotechnology*, vol. 28, no. 8, Feb. 2017, Art. no. 08LT02. doi: 10.1088/1361-6528/aa5838.